Title	Acceptable range of forearm deformity derived from relation to three-dimensional analysis and clinical impairments
Author(s)	Shiode, Ryoya; Miyamura, Satoshi; Kazui, Arisa et al.
Citation	Journal of Orthopaedic Research. 2024, 42(7), p. 1509-1518
Version Type	VoR
URL	https://hdl.handle.net/11094/95275
rights	This article is licensed under a Creative Commons Attribution 4.0 International License.
Note	

RESEARCH ARTICLE

Acceptable range of forearm deformity derived from relation to three-dimensional analysis and clinical impairments

Ryoya Shiode[1] 🔘 | Satoshi Miyamura[1] 🔘 | Arisa Kazui[1] | Toru Iwahashi[1] |
Hiroyuki Tanaka[1] | Seiji Okada[1] | Tsuyoshi Murase[2] 🔘 | Kunihiro Oka[1] 🔘

[1]Department of Orthopaedic Surgery,
Graduate School of Medicine, Osaka
University, Suita, Japan

[2]Department of Orthopaedic Surgery,
BellLand General Hospital, Sakai, Japan

Correspondence
Kunihiro Oka, Department of Orthopaedic
Surgery, Graduate School of Medicine, Osaka
University, 2-2 Yamada-oka, Suita 565-0871,
Japan.
Email: oka-kunihiro@umin.ac.jp

Abstract

This study aimed to investigate deformity patterns that cause clinical impairments and determine the acceptable range of deformity in the treatment of forearm diaphyseal fractures. A three-dimensional (3D) deformity analysis based on computed bone models was performed on 39 patients with malunited diaphyseal both-bone forearm fractures to investigate the 3D deformity patterns of the radius and ulna at the fracture location and the relationship between 3D deformity and clinical impairments. Clinical impairments were evaluated using forearm motion deficit. Cutoff values of forearm deformities were calculated by performing receiver operating characteristic analysis using the deformity angle and the limited forearm rotation range of motion (less than 50° of pronation or supination) resulting in activities of daily living (ADL) impairment as variables. The extension, varus, and pronation deformities most commonly occurred in the radius, whereas the extension deformity was commonly observed in the ulna. A positive correlation was observed between pronation deficit and extension deformity of the radius (R = 0.41) and between supination deficit and pronation deformity of the ulna (R = 0.44). In contrast, a negative correlation was observed between pronation deficit and pronation deformity of the radius (R = −0.44) and between pronation deficit and pronation deformity of the ulna (R = −0.51). To minimize ADL impairment, radial extension deformity should be <18.4°, radial rotation deformity <12.8°, and ulnar rotation deformity <16.6°. The deformities in the sagittal and axial planes of the radius and in the axial plane of the ulna were responsible for the limited forearm rotation.

KEYWORDS
3D deformity analysis, acceptable range of forearm deformity, deformity patterns, forearm diaphyseal fractures

1 | INTRODUCTION

Diaphyseal forearm fractures are prevalent, accounting for 14.9% of pediatric fractures,[1] and their incidence rate is increasing.[2,3] Because fractures in children have a high remodeling ability, conservative treatment is often used for treating fractures. However, when conservative treatment is administered after manual reduction, 34% patients experience redisplacement,[4] which often results in malunion.[5] The forearm has a complex three-dimensional (3D) anatomical bony structure that serves as a functional unit and allows wide rotational movements; thus, disruption of these structures after malunited forearm fractures causes forearm dysfunction, such as limited forearm rotation range of motion (ROM).

Several biomechanical studies using cadavers have revealed that rotational deformity in the forearm bones reduces forearm ROM.[6,7] Some studies also evaluated in vivo forearm rotation deformity using 2D images.[8,9] However, 2D evaluation of rotation deformity is inaccurate,[10] and the relationship between deformity patterns and clinical impairments has not been adequately evaluated. In vivo, research using 3D computed tomography (CT) bone models of various forearm rotational positions has revealed that forearm deformity can limit forearm ROM and cause adjacent joint problems.[11] However, the deformity patterns and the correlation between bone deformity and clinical impairments in cases of malunited diaphyseal both-bone forearm fractures using a statistically sufficient sample have not been reported; moreover, the acceptable range of fracture displacement in vivo, as evaluated using 3D images, remains unknown. In the present study, we aimed to clarify the relationship among deformity patterns, extent of deformity, and clinical impairments in cases of symptomatic malunited diaphyseal both-bone forearm fractures using a sufficient sample and determine the acceptable range of fracture displacement to assist in the initial treatment of diaphyseal forearm fractures.

As a result, we posed the following questions: (1) Is there a specific trend in deformity patterns in individuals with symptomatic malunited diaphyseal both-bone forearm fractures? (2) Is there a statistical association between 3D deformity angles and clinical impairments in the radius and ulna? (3) What is the cutoff value of the 3D deformation angle that interferes with daily activities?

2 | METHODS

This study was approved by the institutional review board of Osaka University Hospital (Approval no. 14179-4); the need for informed consent was waived off due to the retrospective nature of the study. All procedures were performed in accordance with the ethical standards of the responsible committees on human experimentation (institutional and national) and 1975 Declaration of Helsinki, as revised in 2000.

2.1 | Patients

We retrospectively reviewed 207 consecutive patients with malunited forearm fractures who visited our institution and underwent bilateral CT of the forearm for evaluation of bony deformity from August 2002 to March 2022 (Supplement 1). Malunion was defined as angular deformities of >10° compared with the normal side, as measured using radiography.[11] Patients with malunited diaphyseal forearm fractures were included. Diaphysis was defined as the central 60% of the total length of each bone,[11] and fractures in other areas were excluded. In total, 113 patients were identified. Of these, 53 patients with dislocated radial or ulnar heads, 16 patients with isolated radius/ulna fracture, 2 patients aged <10 years in whom future remodeling was expected,[12] 2 patients with bilateral malunited diaphyseal forearm fractures, and 1 patient with the nonunion of the ulna were excluded. Finally, 39 patients were analyzed in this study.

2.2 | 3D bone models

All patients underwent CT scan of the affected and contralateral normal forearms with a low-dose radiation protocol[13] (tube voltage: 120 kV, current: 30 mA, slice thickness: 1.25 mm, and pixel size: 0.48 mm). The patients were asked to lie down in the prone position, with the upper extremity elevated overhead and cervical spine in extension to avoid radiation exposure to the head and trunk. The bilateral 3D surface models of the radius, ulna, and distal humerus were generated from CT data using a commercial software (BoneViewer; Teijin Nakashima Medical Co.).

2.3 | 3D deformity analysis

A mirror image of the contralateral normal bone model was created to analyze the 3D deformity using another commercial computer software (Bone Simulator; Teijin Nakashima Medical Co.). First, the proximal parts of the affected bone and the mirror image of the contralateral normal bone were superimposed by applying the iterative closest point surface-based registration algorithm[14] (Figure 1A). Second, the distal parts were similarly superimposed. The resulting relative displacement matrix was used to evaluate the 3D deformity.

The coordinate system of the radius and ulna was established on the mirror images of the normal bone. For the radius, the coordinate system was set up based on the International Society of Biomechanics (ISB) recommendations.[11,15,16] The y axis was aligned with the long axis of the radius, and the z-axis projected from the base of the concavity of the sigmoid notch toward the radial styloid on the plane perpendicular to the y axis. The x-axis was perpendicular to both the y and z axes. (Figure 1B). Since the ISB system of the ulna depends on the position of the radius, the coordinate system used in previous studies was adopted.[11,15] The y-axis was aligned with the long axis of the ulna. The x-axis was set perpendicular to the y-axis, paralleling to a line passing through the coronoid process. The z-axis was perpendicular to both the y- and x-axes. The origin of the coordinate system was set at
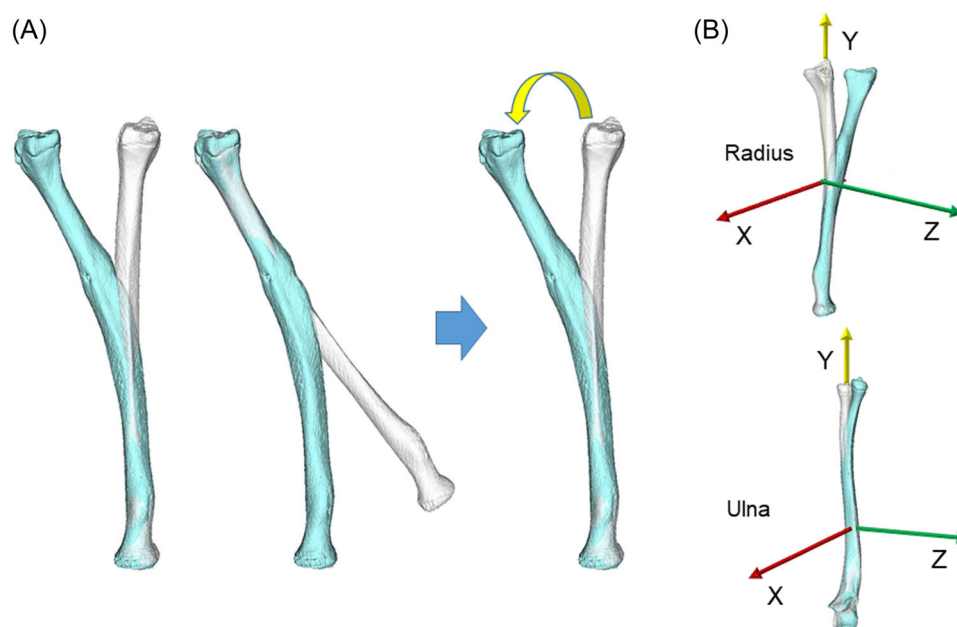
FIGURE 1 Malunited radius (blue) and mirror image of the contralateral normal radius (white). (A) First, the proximal part of the malunited bone is superimposed on the corresponding part of the mirror image of the contralateral, normal bone. Second, the distal part of the malunited bone is superimposed on the corresponding part of the mirror image of the contralateral, normal bone. Finally, the amount of displacement from the proximal superimposed position toward the distal superimposed position was calculated to determine the 3D deformity. (B) The coordinate system of the radius and ulna. Rotation around the X-, Y-, and Z-axes indicates valgus (+) or varus (−), internal rotation (+) or external rotation (−), and extension (+) or flexion (−) deformities, respectively.

the volumetric center of each bone model. The relative displacement matrix described above was quantified in three directions using the Euler angle method with these coordinate systems.[15,17]

Positive and negative sagittal, coronal, and axial angles were defined as extension and flexion, valgus and varus, and pronation and supination, respectively. The location of the deformity was quantified as the percentage of the total length of the bone from the proximal end. The extent of deformity of the radius and ulna in the three directions was compared. Furthermore, the degree of deformity of the radius and ulna was classified into four groups using the greatest deformity angle among the three directions: <10° (group I), 10°–20° (group II), 20°–30° (group III), and >30° (group IV).

2.4 | Clinical impairments

Forearm rotation was measured at the wrist using a goniometer, with the humerus in the vertical position and elbow at 90° of flexion. Differences in total arc, pronation, and supination between the normal and affected sides were defined as total arc, pronation, and supination deficits, respectively.

2.5 | Correlations

The correlation of the location of the deformity between the radius and ulna was examined. Moreover, correlations among the location

of the deformity, amount of deformity, and total arc/pronation/supination deficits were examined. The total arc deficit was compared among the four groups of patients with different degrees of deformity of the radius and ulna.

2.6 | Cutoff value of the 3D deformation angle

Receiver operating characteristic (ROC) analysis was used to define the cutoff value of the 3D deformation angle only for correlations observed between deformity and forearm rotation limitation. Both the radius and ulna were examined for deformations in only major directions in each of the three axes. We analyzed the cutoff values that resulted in less than 50° of pronation or supination as it is thought to cause activities of daily living (ADL) impairment.[18]

2.7 | Statistical analysis

All statistical analyses were performed using the JMP Pro 14 software (SAS). Data were assessed for normal distribution using the Shapiro–Wilk test. Spearman correlation coefficient was used to analyze the relationship of the location between the radius and ulna. The relationship among the location of the deformity, amount of deformity, and total arc/pronation/supination deficits was analyzed using Pearson or Spearman correlation coefficient. The strength of the correlation was classified as slight ($R < 0.2$), low ($R = 0.2$–0.4),

moderate (R = 0.4–0.7), or high (R > 0.7),[19] with moderate or strong correlation defined. For associated factors, ROC curves were also created. Using the Youden index, the area under the curve (AUC) was calculated, and the best cutoff was obtained. The relationship between the extent of deformity and total arc deficit was analyzed using the Tukey–Kramer honestly significant difference test.

To analyze correlations among the location of the deformity, extent of deformity, and total arc/pronation/supination deficits, a priori power analysis ($\alpha = 0.05$, $1 - \beta = 0.8$) was conducted using G-power 3.1 (University of Kiel) to detect correlation coefficients of >0.45.[15] The minimum sample size to identify significant differences was 33 patients.

3 | RESULTS

In total, 39 patients, including 29 men and 10 women, were analyzed. The median age of patients was 16 (IQR, 13–20) years. The median period from the original injury to CT imaging was 31 (IQR, 11–61) months. Cast immobilization was performed in 30 patients, whereas percutaneous pinning was performed in 9 patients. A total of 36 patients had limited forearm rotation ROM, and 3 patients had adjacent joint problems.

3.1 | Trends in deformity patterns in patients with symptomatic malunited diaphyseal both-bone forearm fractures

The distribution of combinations of deformity patterns in three directions is summarized in Table 1. In the radius, a pattern with extension, varus, and pronation accounted for one-third of the total pattern (Figure 2). In each deformity direction, extension (n = 33, 85%), varus (n = 24, 62%), and pronation (n = 25, 64%) were common. Flexion deformities (n = 6) were accompanied by pronation deformities (n = 6, 100%), and supination deformities (n = 14) were accompanied by extension deformities (n = 14, 100%). In the ulna, the overall pattern of deformity varied, but extension deformities (n = 25, 64%) were often present.

The distribution of cases by the extent of deformity in three directions is shown in Figure 3. In the sagittal direction, the median deformity angle was 14° (IQR, 10.2°–24°) in the radius, which was significantly greater than that in the ulna (6° [IQR, 2.4°–9.6°]) (p < 0.001). In the coronal direction, the median deformity angle was 5° (IQR, 3.6°–8.8°) and 8° (IQR, 5.4°–10.8°) in the radius and ulna, respectively (p = 0.14). In the axial direction, the median deformity angle was 15° (IQR, 5.6°–28.6°) and 12° (IQR, 3.9°–18.8°) in the radius and ulna, respectively (p = 0.14).

The median location of the deformity of the radius and ulna was 49% and 61%, respectively, which had a positive correlation between them (R = 0.66; p < 0.001). No correlation was noted between the location of the deformity and deformity directions in the radius and ulna. However, for the radius, cases with >20° axial plane deformity were deformed at the proximal and middle portion (no significant

TABLE 1 Three-dimensional deformity patterns in the radius and ulna and the number of patients.

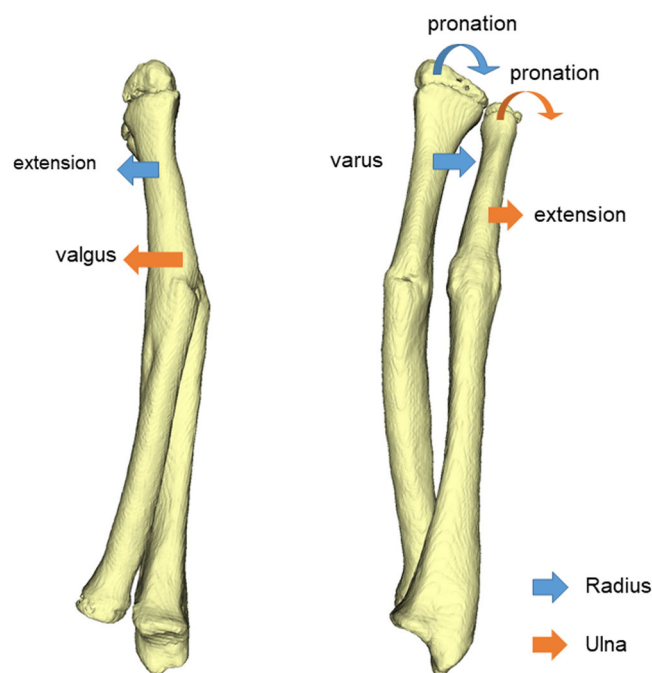| Radius; N = 39			
Extension	Valgus	Pronation	6
		Supination	7
	Varus	Pronation	13
		Supination	7
Flexion	Valgus	Pronation	2
		Supination	0
	Varus	Pronation	4
		Supination	0
Ulna; N = 39			
Extension	Valgus	Pronation	8
		Supination	5
	Varus	Pronation	6
		Supination	6
Flexion	Valgus	Pronation	5
		Supination	5
	Varus	Pronation	3
		Supination	1

FIGURE 2 Typical deformity in malunited forearm diaphyseal fractures. The radius was deformed in the direction of extension, varus, and pronation. The ulna was deformed in the direction of extension, valgus, and pronation.
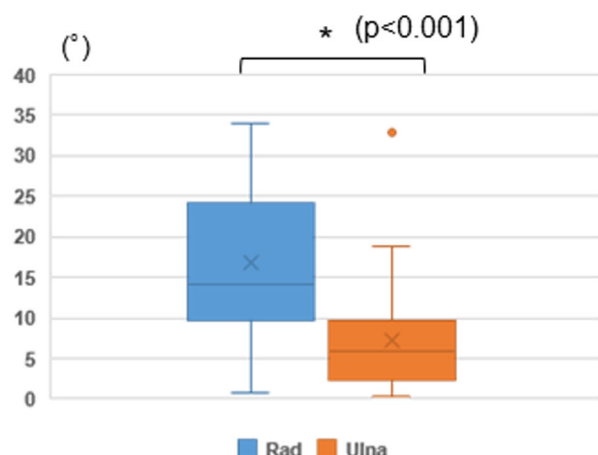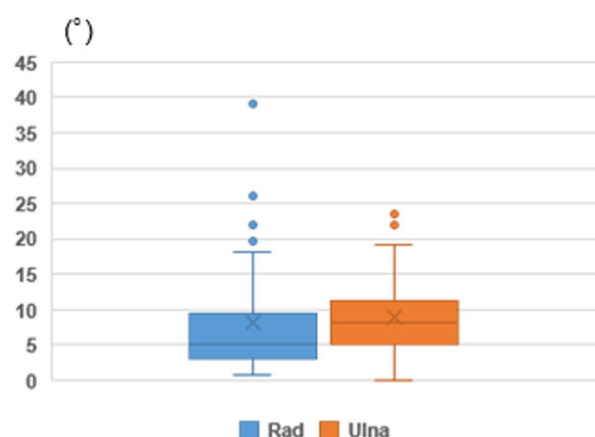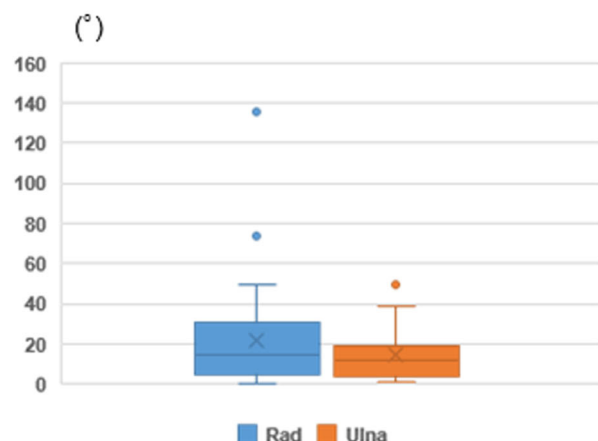
FIGURE 3   Relationship of the extent of deformity between the radius and ulna in three directions. The radius remains significantly more deformed in the sagittal plane than in the ulna.

difference was observed in the deformity between the proximal and middle and distal portions [$p = 0.92$]). For the ulna, cases with >20° axial plane deformity were deformed at the distal portion (no significant difference was observed in the deformity between the proximal and middle and distal portions [$p = 0.22$]) (Figure 4). Cases with >20° sagittal deformity were not characterized based on the deformity location. The degree of deformities of the sagittal plane in the ulna and coronal plane in the radius and ulna were not severe, with the degree of most deformities being <20°.

3.2 | Relationship between 3D deformity angles and clinical impairments in the radius and ulna

The median total arc, pronation, and supination deficits were 90° (IQR, 62.5°–110°), 40° (IQR, 12.5°–60°), and 40° (IQR, 5°–87.5°),

respectively. Positive correlations were found between pronation deficit and extension deformity of the radius (R = 0.41; $p = 0.001$), supination deficit and pronation deformity of the radius (R = 0.65; $p < 0.001$), total arc deficit and pronation deformity of the radius (R = 0.41; $p = 0.009$), and supination deficit and pronation deformity of the ulna (R = 0.44; $p = 0.005$). Negative correlations were observed between pronation deficits and pronation deformity of the radius (R = −0.44; $p = 0.005$) and ulna (R = −0.51; $p = 0.001$) (Figures 5 and 6, Supplement 2 and 3). No correlations were observed between the location of the deformity and forearm motion in either total arc deficit, pronation deficit, or supination deficit.

In the radius, no cases belonged to group I (Figure 7). The median total arc deficits were 87.5° (IQR, 35°–102.5°), 95° (IQR, 65°–110°), and 95° (IQR, 87.5°–125°) in groups II, III, and IV, respectively. In the ulna, the median total arc deficits were 75° (IQR, 42.5°–90°), 110° (IQR, 90°–120°), 100° (IQR, 97.5°–100°), and 80° (IQR, 62.5°–97.5°) in
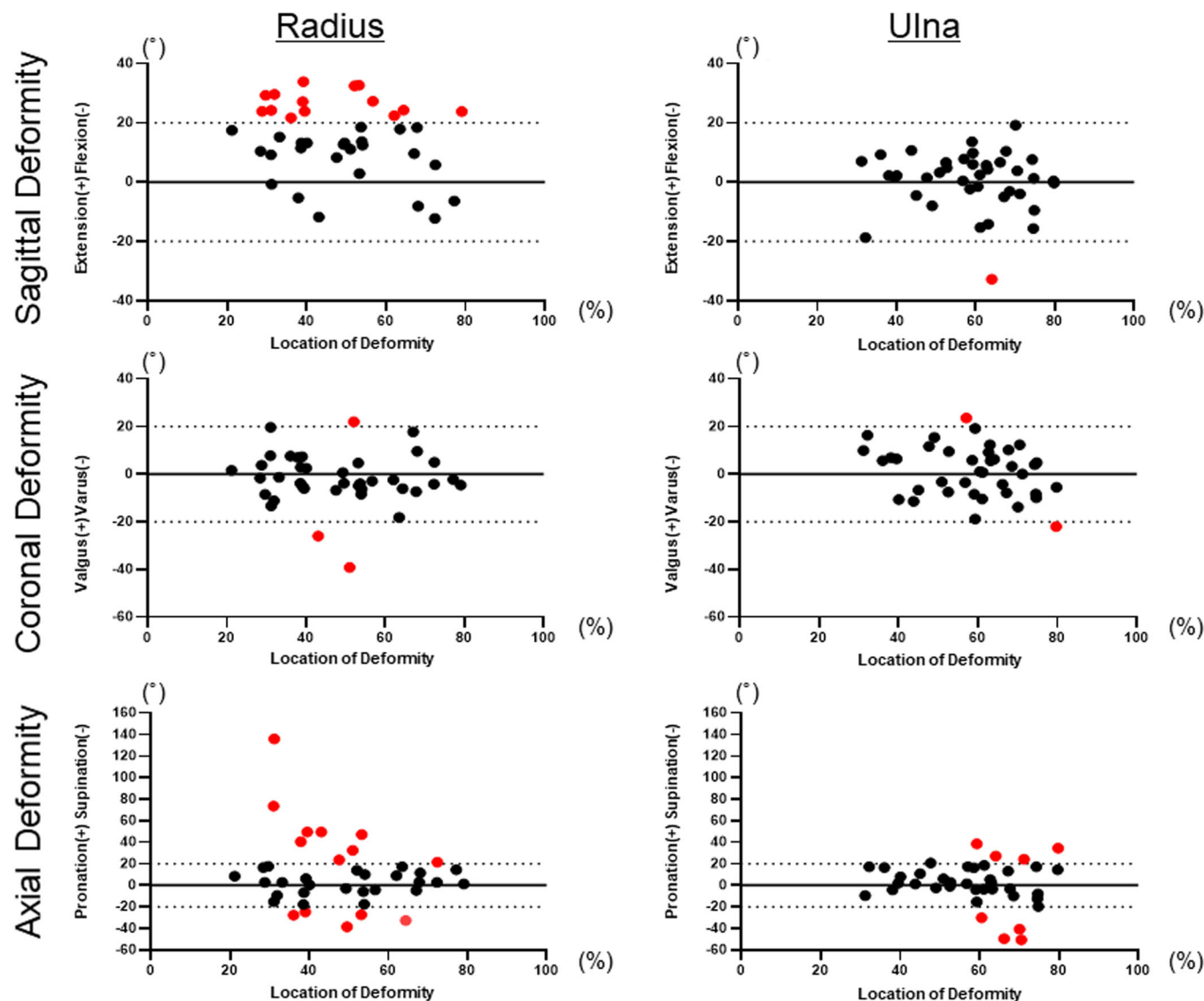
FIGURE 4 Relationship between the location of the deformity and deformity directions in the radius and ulna. Examples of deformities of ≥20° within each deformity are indicated by red dots. The axial deformity of the radius shows a considerable deformity proximally, whereas the axial deformity of the ulna shows a considerable deformation distally.

groups I, II, III, and IV, respectively. The total arc deficit in group I was significantly smaller than that in groups II (p = 0.01) and IV (p = 0.03).

3.3 | Cutoff value of the 3D deformation angle interfering with ADL

Cutoff values for forearm deformities that resulted in ADL impairment were determined using ROC analysis. Deformities with an extension deformity in the radius of ≥18.4° (AUC = 0.76; 95% CI for AUC = 0.59–0.92; p = 0.012) limited the pronation to <50° (Figure 8). Pronation deformity in the radius of ≥12.8° (AUC = 0.67; 95% CI for AUC = 0.42–0.91; p = 0.17) and pronation deformity in the ulna of ≥16.6° (AUC = 0.69; 95% CI for AUC = 0.45–0.93; p = 0.13) limited supination to <50°.

4 | DISCUSSION

Regarding the three questions posed in this study, we got the following important findings. Regarding question (1), the extension, varus, and pronation deformities most commonly occurred in the radius, whereas the extension deformity was commonly observed in the ulna. Regarding question (2), a positive correlation was observed between pronation deficit and extension deformity of the radius (R = 0.41) and supination deficit and pronation deformity of the ulna (R = 0.44). A negative correlation was observed between pronation deficit and pronation deformity of the radius (R = −0.44) and pronation deficit and pronation deformity of the ulna (R = −0.51). Regarding question (3), the cutoff values for forearm deformity resulting in ADL impairment are extension deformity in the radius of ≥18.5° leading to pronation limitation, pronation deformity in the
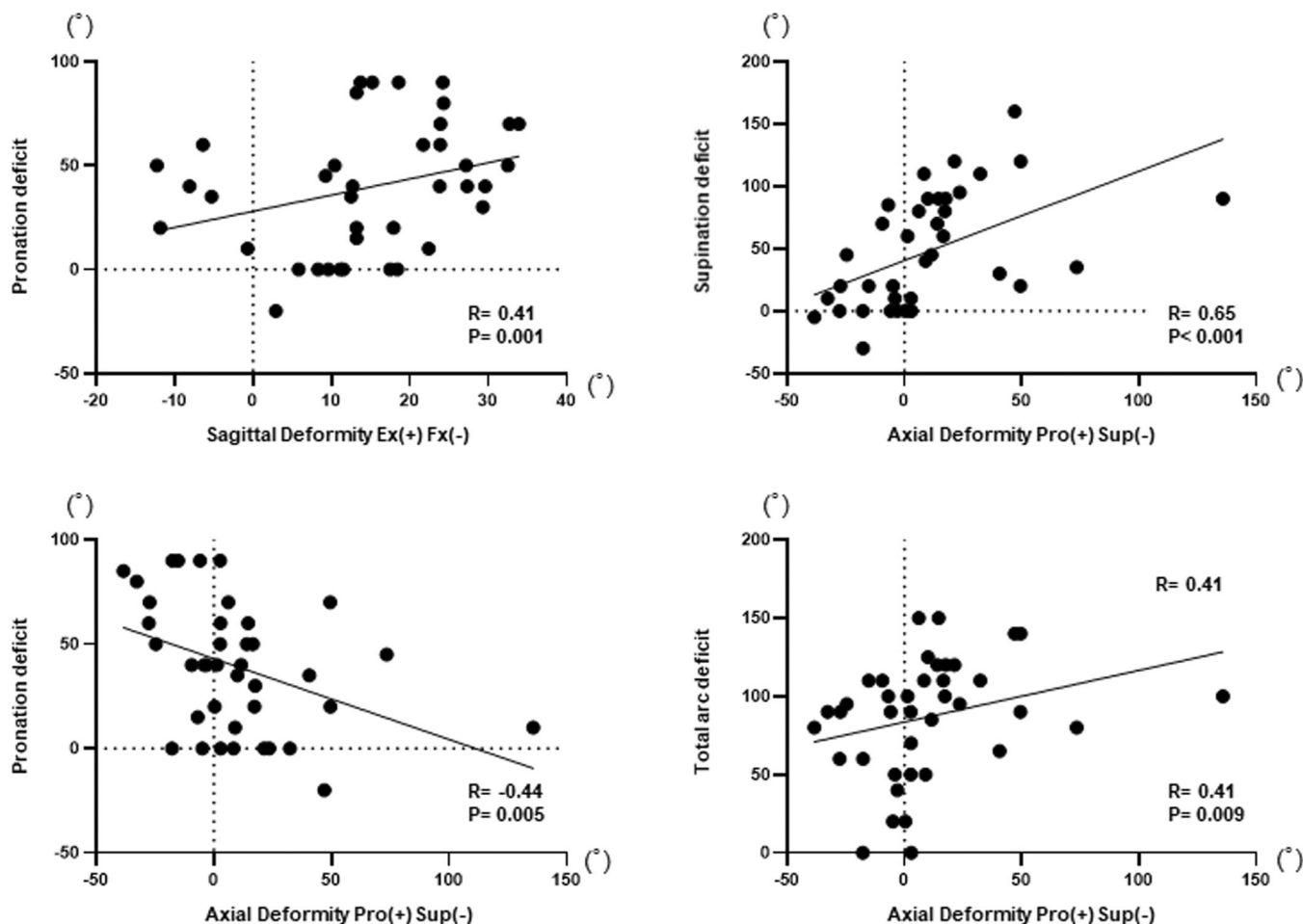
Radius

FIGURE 5 Correlations between deformity directions in the radius and forearm motion deficit. There is a positive correlation between pronation limitation and extension deformity of the radius, pronation limitation and pronation deformity of the radius, and limitation of the full ROM and pronation deformity of the radius. There is a negative correlation between the pronation limitation and the pronation deformity of the radius.

radius of ≥12.8°, and pronation deformity in the ulna of ≥16.5° leading to supination limitation.

Malunion of forearm fractures may decrease the ROM of forearm rotation.[20] In forearm deformities, which often include rotational deformity,[15] simple angulation and translation of the radius and ulna can be accurately detected using plain radiography; however, rotational deformities cannot be measured using plain radiography. Therefore, understanding the 3D pattern of malunited diaphyseal forearm fractures deformity and determining the relationship between the deformity and ROM restriction in diaphyseal forearm fractures are essential for the initial treatment. Accordingly, we investigated the relationship among the deformity pattern, extent of deformity, and clinical impairments of malunion of diaphyseal forearm fractures.

Our 3D deformity analysis showed that one-third malunion of the radius had characteristic deformity patterns of extension, varus, and pronation, whereas those of the ulna had various deformity

patterns. This characteristic deformity pattern[15] and patterns such as always pronation when it was flexion and always extension when it was supination in the radius could be influenced by the displacement at the initial injury. Extension deformity is common in the radius, as the attachment of the biceps brachii to the proximal fragment causes relative displacement of the distal fragment in the extension direction. Axial forces on the curved shape of the radius and load on the curvature may cause varus deformity. The pronation deformity could be caused by the forces of the supinator muscle to the proximal fragment and of the pronator teres and pronator quadratus muscle to the distal fragment. These characteristic patterns could provide useful information to prevent recurrent displacement during conservative treatment. In addition, significant restriction of forearm rotation was reported to be caused by forearm angulated with 10°–15° in clinical cases[4,21] and rotational deformity with ≥10° in a cadaveric study[6,7] In the present study, the patients had radial and ulnar deformities in three directions, the radius was
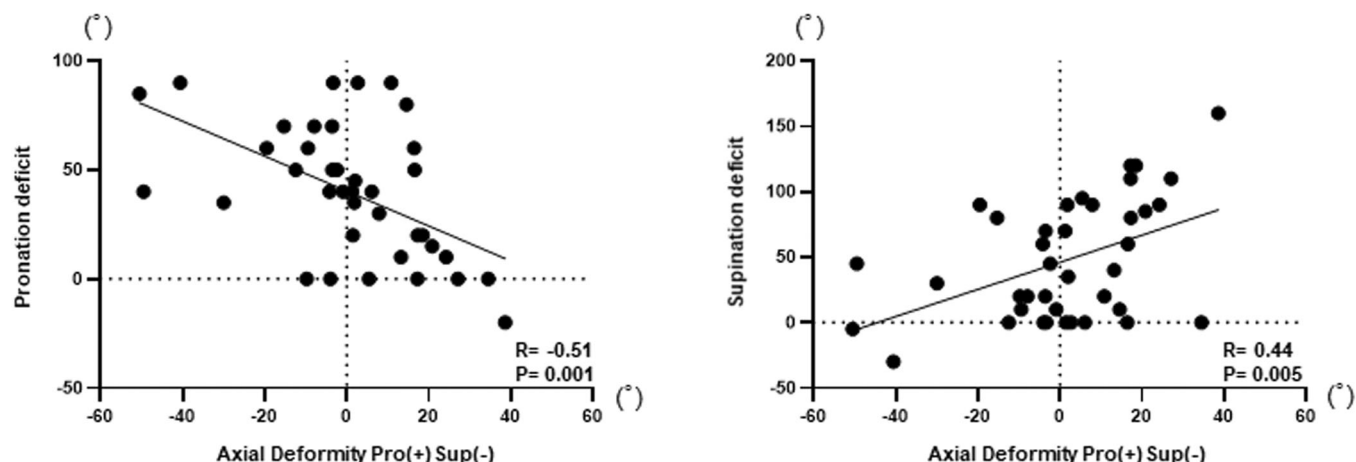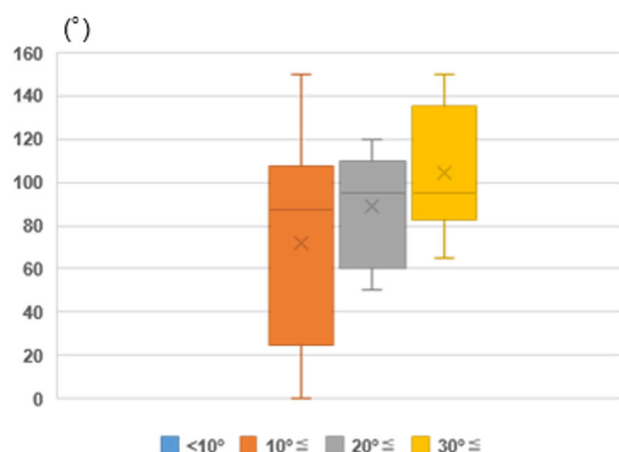
FIGURE 6 Correlations between deformity directions in the ulna and forearm motion deficit. There is a positive correlation between supination limitation and pronation deformity of the ulna. There is a negative correlation between the pronation limitation and the pronation deformity of the ulna.
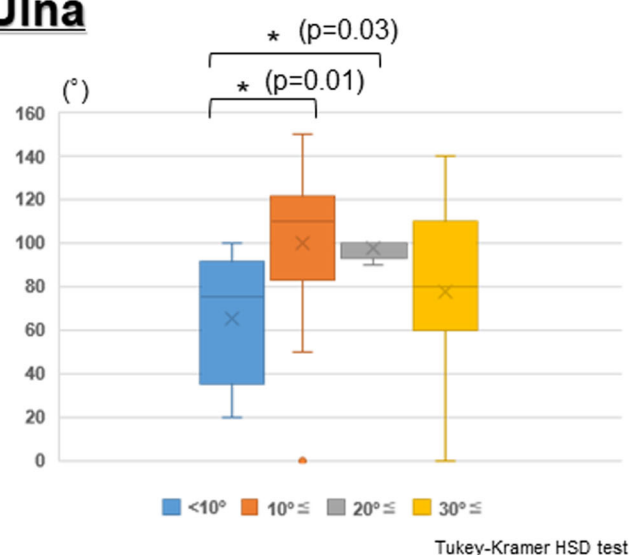

FIGURE 7 Relationships between the amount of deformity and total arc deficit. There were no cases with a radius <10°. As the radial and ulnar deformity increased, ROM limitations tended to increase.

deformed greatly in the sagittal and axial directions and the ulna in the axial direction. This is consistent with the pattern of deformities reported in a previous study.[15] These directions of deformity should be considered during the initial treatment.

A strong correlation was observed between radial and ulnar deformity locations, but no correlation was observed between deformity location and deformity pattern in three directions. However, axial deformity was greater on the proximal and middle side of the radius and the distal side of the ulna, as the proximal radius was supinated by the forces of the supinator muscle and the biceps tendon and the distal radius was pronated by those of the pronator muscles.[15,22] Meanwhile, the distal ulna was supinated by

the force of the pronator quadratus muscle. Attention should be paid to the rotation deformities in the radius and ulna if the fractures are proximal and distal, respectively.

The deformity of the radius was significantly greater than that of the ulna in the sagittal plane. The underlying reason for this observation is unclear; however, one reason could be that the intervening external stress is applied to the radius rather than to the ulna when the fracture is inflicted with the hand extended. The coronal deformity of the radius was significantly smaller than the sagittal deformity, probably attributing to the anatomy of the radius. In the coronal plane, the radius is stabilized by the annular ligament at the proximal radioulnar joint, interosseous ligament at the diaphysis,
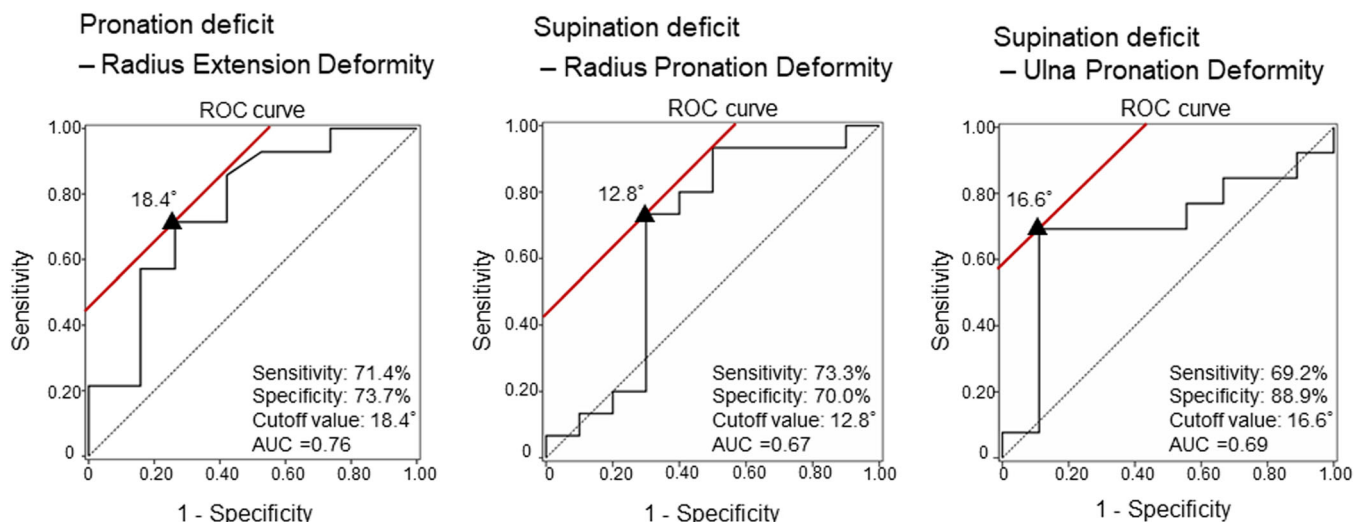
FIGURE 8 ROC curves in pronation limitation and radial extension deformity, supination limitation and radial pronation deformity, supination limitation, and ulnar pronation deformity.

and distal radioulnar ligament at the distal radioulnar joint. However, the radial stabilizer is absent in the sagittal plane.

In the correlation analysis between deformity pattern and forearm motion deficit, a positive correlation was observed between the extension deformity of the radius and pronation deficit. This suggests that an extension deformity of the radius may cause bony impingement between both bones at pronation[11] (Supplement 4). Moreover, the pronation deficit was small and the supination deficit was large in the radial pronation deformity. The full ROM shifted to pronation due to the pronation deformity, resulting in supination restriction.

In the analysis of the relationship between the extent of deformity and total arc deficit, no cases belonged to group I in the radius. Patients with radial deformity of ≤10° were probably not included in this study because their ulnar deformity was small, they had no clinical issues, and they did not visit a hospital. In groups III and IV, the deformity was >20°, and a large total arc deficit was observed in most cases, whereas in group II, the deformity was 10°–20°, and a small total arc deficit was observed only in some cases. Although no statistically significant differences were observed in the radius, the total arc deficit tended to increase as the extent of deformity increased. This suggests the importance of reducing the deformity in all three directions as small as possible, especially <10°.

In this study, the cutoff value for extension deformity in the radius leading to pronation limitation and resulting in ADL impairment was ≥18.4°, and although not significantly, pronation deformity in the radius of ≥12.8° and pronation deformity in the ulna of ≥16.6° led to supination limintation and consequently ADL impairment. Previous investigations using cadavers have shown that angular abnormalities of ≥15°[6,7] and rotational malformations of ≥30°[23,24] significantly impede the forearm ROM. The cutoff values for angular deformations in the present study are comparable to those in the cadaver study,[6,7] but for rotational deformity, the results suggest that smaller deformity than previously reported may cause forearm

rotation limitation. To the best of our knowledge, this is the first study to demonstrate a cutoff value for forearm rotation deformity leading to in vivo forearm rotation limitation. The discrepancy between this study and the previous cadaver study could be attributed to the inclusion of characteristic deformity patterns due to actual fractures and soft tissue tension's significant role in forearm rotational motion.

4.1 | Limitations

This study has several limitations. First, this study did not consider the condition of the soft tissues surrounding the forearm, such as muscles, ligaments, and joint capsules. Second, the study only included patients with severe deformity, as patients with insufficiency fractures of the forearm without rotational restriction generally do not seek medical care.

5 | CONCLUSIONS

In malunited diaphyseal forearm fractures, the radius tends to have extension, varus, and pronation deformities, and the combination of these deformities accounts for one-third of the total deformities. Special attention should be paid to the deformities in the radius in the sagittal and axial planes. The ulna exhibits various deformity patterns, but attention should be paid to the pronation deformity. To minimize ADL impairment, radial extension deformity should be <18.4°, radial rotation deformity <12.8°, and ulnar rotation deformity <16.6°.

AUTHOR CONTRIBUTIONS

All authors contributed to the conception and design of the study, were involved in drafting the article critically for important intellectual

CONFLICT OF INTEREST STATEMENT

Each author certifies that there are no funding or commercial associations (consultancies, stock ownership, equity interest, patent/ licensing arrangements, etc.) that might pose a conflict of interest in connection with the submitted article related to the author or any immediate family members.

ORCID

Ryoya Shiode https://orcid.org/0000-0002-3148-0399
Satoshi Miyamura https://orcid.org/0000-0002-2245-5554
Tsuyoshi Murase http://orcid.org/0000-0001-5628-5891
Kunihiro Oka http://orcid.org/0000-0002-7770-4634

REFERENCES

1. Cheng JCY, Ng BKW, Ying SY, Lam PKW. A 10-year study of the changes in the pattern and treatment of 6,493 fractures. *J Pediatr Orthop*. 1999;19:344-350.
2. Grahn P, Sinikumpu JJ, Nietosvaara Y, et al. Casting versus flexible intramedullary nailing in displaced forearm shaft fractures in children aged 7-12 years: a study protocol for a randomised controlled trial. *BMJ Open*. 2021;11:e048248.
3. Kapila R, Sharma R, Chugh A, Goyal M. Evaluation of clinical outcomes of management of paediatric bone forearm fractures using titanium elastic nailing system: a prospective study of 50 cases. *J Clin Diagn Res*. 2016;10:RC12-RC15.
4. Colaris JW, Allema JH, Biter LU, et al. Conversion to below-elbow cast after 3 weeks is safe for diaphyseal both-bone forearm fractures in children. *Acta Orthop*. 2013;84:489-494.
5. Colaris JW, Oei S, Reijman M, Holscher H, Allema JH, Verhaar JAN. Three-dimensional imaging of children with severe limitation of pronation/supination after a both-bone forearm fracture. *Arch Orthop Trauma Surg*. 2014;134:333-341.
6. Matthews LS, Kaufer H, Garver DF, Sonstegard DA. The effect on supination-pronation of angular malalignment of fractures of both bones of the forearm. *J Bone Jt Surg*. 1982;64:14-17.
7. Tarr RR, Garfinkel AI, Sarmiento A. The effects of angular and rotational deformities of both bones of the forearm. An in vitro study. *J Bone Jt Surg*. 1984;66:65-70.
8. Bindra RR, Cole RJ, Yamaguchi K, et al. Quantification of the radial torsion angle with computerized tomography in cadaver specimens. *J Bone Jt Surg*. 1997;79:833-837.
9. Creasman C, Zaleske DJ, Ehrlich MG. Analyzing forearm fractures in children. The more subtle signs of impending problems. *Clin Orthop Relat Res*. 1984;188:40-53.
10. Nagy L, Jankauskas L, Dumont CE. Correction of forearm malunion guided by the preoperative complaint. *Clin Orthop Relat Res*. 2008; 466:1419-1428.
11. Abe S, Murase T, Oka K, Shigi A, Tanaka H, Yoshikawa H. In vivo three-dimensional analysis of malunited forearm diaphyseal fractures with forearm rotational restriction. *J Bone Jt Surg*. 2018;100:e113.
12. Truntzer J, Vopat ML, Kane PM, Christino MA, Katarincic J, Vopat BG. Forearm diaphyseal fractures in the adolescent population: treatment and management. *Eur J Orthop Surg Traumatol*. 2015;25:201-209.
13. Oka K, Murase T, Moritomo H, Goto A, Sugamoto K, Yoshikawa H. Accuracy analysis of three-dimensional bone surface models of the forearm constructed from multidetector computed tomography data. *Int J Med Robot Comput Assist Surg*. 2009;5:452-457.
14. Besl PJ, McKay ND. A method for registration of 3-D shapes. *IEEE Trans Pattern Anal Mach Intell*. 1992;14:239-256.
15. Miyake J, Oka K, Kataoka T, Moritomo H, Sugamoto K, Murase T. 3-Dimensional deformity analysis of malunited forearm diaphyseal fractures. *J Hand Surg [Am]*. 2013;38:1356-1365.
16. Wu G, van der Helm FCT, (DirkJan) Veeger HEJ, et al. ISB recommendation on definitions of joint coordinate systems of various joints for the reporting of human joint motion—part II: shoulder, elbow, wrist and hand. *J Biomech*. 2005;38:981-992.
17. Abe S, Oka K, Miyamura S, et al. Three-dimensional in vivo analysis of malunited distal radius fractures with restricted forearm rotation. *J Orthop Res*. 2019;37(9):1881-1891.
18. Morrey BF, Askew LJ, Chao EY. A biomechanical study of normal functional elbow motion. *J Bone Jt Surg*. 1981;63:872-877.
19. Guilford JP. *Fundamental statistics in psychology and education*. 2nd ed. McGraw-Hill; 1950.
20. Bauer DE, Zimmermann S, Aichmair A, et al. Conventional versus computer-assisted corrective osteotomy of the forearm: a retrospective analysis of 56 consecutive cases. *J Hand Surg [Am]*. 2017; 42:447-455.
21. Price CT. Acceptable alignment of forearm fractures in children: open reduction indications. *J Pediatr Orthopaed*. 2010;30:S82-S84.
22. Cruess RL. The management of forearm injuries. *Orthop Clin North Am*. 1973;4:969-982.
23. Dumont CE, Thalmann R, Macy JC. The effect of rotational malunion of the radius and the ulna on supination and pronation. *J Bone Joint Surg Br*. 2002;84:1070-1074.
24. Kasten P, Krefft M, Hesselbach J, Weinberg AM. How does torsional deformity of the radial shaft influence the rotation of the forearm? A biomechanical study. *J Orthop Trauma*. 2003;17:57-60.

SUPPORTING INFORMATION

Additional supporting information can be found online in the Supporting Information section at the end of this article.

How to cite this article: Shiode R, Miyamura S, Kazui A, et al. Acceptable range of forearm deformity derived from relation to three-dimensional analysis and clinical impairments. *J Orthop Res*. 2024;1-10. doi:10.1002/jor.25805